Correia, DM.; Costa, CM.; Rodriguez-Hernandez, J.; Tort-Ausina, I.; Teruel Biosca, L.; Torregrosa Cabanilles, C.; Meseguer Dueñas, JM.... (2021). Crystallization Monitoring of Semicrystalline Poly(vinylidene fluoride)/1-Ethyl-3-methylimidazolium Hexafluorophosphate [Emim][PF6] Ionic Liquid Blends. Crystal Growth & Design. 21(8):4406-4416. https://doi.org/10.1021/acs.cgd.1c00333

Crystallization Monitoring of Semicrystalline Poly(vinylidene) Fluoride/ 1-ethyl-3-methylimidazolium Hexafluorophosphate [Emim][PF_6] Ionic Liquid Blends

Daniela M. Correia[1,2], Carlos M. Costa[2,3*], José C. Rodríguez Hernández[4], Isabel Tort-Ausina[4], Laura Teruel Biosca[4], Constantino Torregrosa Cabanilles[4], José Meseguer-Dueñas[4,5], Ivan Krakovsky[6], Senentxu Lanceros-Méndez[7,8], José Luis Gómez Ribelles[4,5]

[1]Centre of Chemistry, University of Trás-os-Montes e Alto Douro, 5000-801Vila Real, Portugal

[2]Centre of Physics, Universidade do Minho, 4710-057 Braga, Portugal

[3]Institute of Science and Innovation for Bio-Sustainability (IB-S), University of Minho, 4710-053 Braga, Portugal

[4]Centre for Biomaterials and Tissue Engineering, CBIT, Universitat Politècnica de València, 46022 Valencia, Spain

[5]Biomedical Research Networking Center on Bioengineering, Biomaterials and Nanomedicine (CIBER-BBN), Valencia, Spain

[6]Department of Macromolecular Physics, Charles University V Holešovičkách 2, 180 00 Prague 8, Czech Republic.

[7]BCMaterials, Basque Center for Materials, Applications and Nanostructures, UPV/EHU Science Park, 48940 Leioa, Spain

[8]IKERBASQUE, Basque Foundation for Science, 48009, Bilbao, Spain

KEYWORDS**:** PVDF; [Emim][PF_6]; electroactive, DSC, β-phase, crystallization kinetics

---

* **Corresponding Authors**

C.M. Costa (cmscosta@fisica.uminho.pt)

ABSTRACT: The electroactive characteristics of poly(vinylidene fluoride) (PVDF) are widely and increasingly being used in technological applications, where controlling the crystallization of the PVDF is of utmost importance. The nucleation and growth of crystals in the β or γ electroactive phases, or in the non-electroactive α phase, depends on a number of factors that, despite the studies carried out, are still to be properly understood, in particular, when blended with specific active fillers. In this context, the crystallization of PVDF blended with the ionic liquid (IL) [Emim][PF_6] has been analyzed. Both components are capable of crystallizing from the melt. The growth of the crystalline phases of PVDF during isothermal crystallization at different temperatures has been monitored using FTIR spectroscopy. The isothermal crystallization kinetics of PVDF and the melting temperatures of both PVDF and the IL were characterized by differential scanning calorimetry and the microstructure of the blends analyzed by optical and electron microscopy. It is observed for [Emim][PF_6]/PVDF blends that the isothermal crystallization from the melt between 120 and 162 ºC produces PVDF crystallites in the β and γ electroactive phases, while the formation of α–phase crystals is nearly suppressed. The morphology of the blends is altered by the IL addition being observed a solid phases separation at room temperature. In addition, [Emim][PF_6] remains liquid when mixed with the amorphous PVDF chains due to the cryoscopic descent.

1. INTRODUCTION

In the context of Industry 4.0, the development of smart materials based on polymer composites and blends is important for a wide variety of areas such as sensors, actuators, biomedicine, environmental and energy applications, as they combine the excellent properties of the polymeric matrix and also of fillers [1-2].

Smart materials are those which properties can be controlled by external physical stimuli, and electroactive polymers, including piezo-, pyro- and ferroelectric ones, have special relevance considering their properties such as low density, excellent mechanical properties, and flexibility. Piezoelectric polymers present moderate piezoelectric coefficient compared to the higher values of piezoelectric ceramics, while the polymer segmental mobility and permanent dipolar moments provide them with high mechanical losses, and a wide variety of dielectric constants. Further, they can be fabricated in a wide variety of shapes using different techniques [3-4].

Poly(vinylidene fluoride) (PVDF) stands out from the other piezoelectric polymers (nylon-9, poly (b-hydroxybutyrate) (PHB), poly[3-hydroxybutyrate- co-3-hydroxyvalerate] (PHBV), poly-L-lactic acid (PLLA), among others) due to its high value of the dielectric constant ($\varepsilon > 7$) and piezoelectric coefficient ($d_{33} \sim -30$ pC / N) [4-5]. PVDF is widely used for the development of smart composite materials [6]. It is a semicrystalline polymer that crystallizes in a spherulitic structure composed of crystalline and amorphous regions and can crystallize in five crystalline structures (α, β, γ, δ and ε) [5, 7-8]. α and β-phases are the most relevant ones for technological applications: while the α-phase is obtained by cooling from the melt, and it is also a thermodynamically more stable phase when the crystallization occurs from the solution at temperatures above 100 ºC [7], the β-phase is obtained by cold straining of films in α-phase, from the solution in certain solvents at low temperatures and by crystallization in the presence of specific fillers [9].

The β-phase is characterized by having electroactive properties (piezo-, pyro- and ferroelectric properties) and it is the most attractive phase from the technological point of view in the areas of sensors and actuators [10-12].

Composites with PVDF matrix have been prepared with different fillers such as conductive particles of carbonaceous materials, ceramic materials such as barium titanate ($BaTiO_3$), magnetic materials such as cobalt ferrite ($CoFe_2O_4$), and different ionic liquids (ILs) among others with the purpose of increasing mechanical, thermal, electric and dielectric properties, as well as to increase or induce functional response for a broad range of applications [4].

In recent years, the properties of ILs have been exploited to obtain PVDF matrix composites for different applications, such as sensors and actuators, batteries, filtration, energy storage devices and biomedical applications [13]. Particular properties of ILs are moderate viscosity, high ionic conductivity, low vapor pressure, and high thermal stability, among others [14-15]. Those particular properties of the ILs allow the obtention of specific dielectric, conductive, and magnetic properties in the composites, depending on the selection of the cation and anion of the IL.

Different ILs varying the anion and cation have been studied as fillers in PVDF based composites, such as 1-ethyl-3-methylimidazolium bis(trifluoromethylsulfonyl) imide, [Emim] [TFSI], 1-ethyl-3-methylimidazolium hexafluorophosphate [Emim][PF_6], 1-ethyl-3-methylimidazolium ethylsulfate [Emim][C_2SO_4], N,N,N-trimethyl-N-(2-hydroxyethyl)ammonium bis-(trifluoromethylsulfonyl)imide [N1112OH][TFSI], trihexyl(tetradecyl)phosphonium bis(trifluoromethylsulfonyl)-imide [P66614][TFSI], and 1-butyl-1-methylpyrrolidinium bis(trifluoromethanesulfonyl)imide [C4C1Pyrr][TFSI] with a focus on the study of the physical-chemical properties,

including mechanical and electrical ones, on the formation of the electroactive β-phase or in the development of specific applications [16-17].

It has been observed that the addition of the IL to the PVDF polymer matrix modifies both local and segmental mobility of the amorphous PVDF chains concluding that PVDF chain segments and IL molecules are mixed at the nanometer range [16].

When crystallization occurs from a mixture of PVDF with a low molecular weight substance, the phase in which the crystals nucleate is modified with respect to crystallizing from the melt due to the enhanced mobility of the chains, which gives them a greater capacity for conformational rearrangements than in the pure polymer. On the other hand, it strongly depends on the specific interaction between the solvent and the PVDF chain segments. Thus, the β-phase is formed from a solution of PVDF in various solvents, in specific temperature intervals, when the solvent evaporates [9]. In the case of crystallization from mixtures of PVDF with an IL, various situations are found depending on the chemical structure of the IL, which justifies the interest of deepening the knowledge of the role that this structure plays in the formation of the crystals of PVDF.

The formation of the electroactive β-phase depends on the anion and cation type and the IL 1-ethyl-3-methylimidazolium chloride [Emim][Cl] has been shown [17] to be a particularly effective IL for the formation of this crystalline form and considering these results, crystallization kinetics of PVDF from the melt in mixtures with [Emim][Cl] have been studied [18]. Nucleation of PVDF in the β-phase has been induced by the presence of [Emim][Cl] under thermal conditions in which neat PVDF crystallizes in the α-phase. Further, it has been observed that the IL remains in the spaces between PVDF lamellae and between spherulites.

Studies of crystallization in β-phase in other mixtures of piezoelectric polymers and ILs are also found in the literature, such as PVDF blended with 1-hexyl-3-methylimidazolium chloride, [Hmim][Cl]) [19] and poly(vinylidene fluoride)-hexafluoropropylene (PVDF-HFP) with N-diethyl-N-(2-methacryloylethyl)-N-methylammonium bis(trifluoromethylsulfonyl) imide ([Demm][TFSI]) [20].

In this context, the goal of the present work is to study the crystallization kinetics of PVDF in a mixture with [Emim][PF_6], the interest in this particular blend being related to the broad use of the PF_6 cation in the lithium hexafluorophosphate salt in lithium-ion cells. Isothermal crystallization in a broad temperature interval is studied by using differential scanning calorimetry (DSC), optical microscopy (OM) and Fourier Transform Infrared Spectroscopy (FTIR). The morphology of these blends is also evaluated.

2. EXPERIMENTAL

2.1.Materials

Poly(vinylidene fluoride), PVDF 6020 (M_w = 670 – 700 kDa), N,N-dimethylformamide (DMF) and 1-ethyl-3-methylimidazolium hexafluorophosphate, [Emim][PF_6] with a purity of 99% were acquired from Solvay, Merck and Iolitec, respectively. The chemical structures of PVDF and IL are represented in Scheme 1.

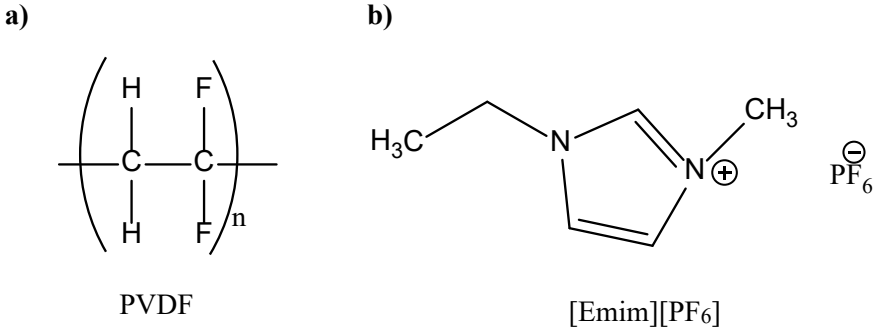

PVDF [Emim][PF_6]

Scheme 1. Chemical Structure of a) PVDF and b) [Emim][PF_6].

2.2.Sample preparation

PVDF/IL films were prepared by casting from a solution in DMF, following the general guidelines presented in previous literature [9]. In a fist stage, PVDF was dissolved in DMF with a concentration of 15 wt% for 3 hours at 25 ºC under magnetic stirring. After the complete dissolution of the polymer, the IL was added to the solution, with an IL/polymer ratio ranging from 5 up to 40% (w/w) and magnetically stirred for 1 hour at 25 ºC until complete homogenization of the polymer and IL is achieved. After this step, the solution was spread on a glass plate and solvent evaporation occurred at 210 °C in an air oven (P-Selecta) for 15 minutes. PVDF/IL films were obtained with a thickness of ~ 50 µm (digital

micrometer Mitutoyo 293-348-30) regardless of the IL concentration. The samples will be identified by the IL content.

2.3.Characterization techniques

The morphology of the PVDF/IL films was examined with a field emission scanning electron microscope (FESEM; ZEISS Ultra-55) at 30 kV, 500 pA, after the deposition of a conductive layer of sputtered platinum. Besides, X-ray microanalysis mapping was performed with an energy dispersive X-ray spectrometer from Oxford Instruments attached to the FESEM. The exposure time of data acquisition was set at 4 minutes for each sample.

Differential Scanning Calorimetry (DSC) was carried out with a DSC 8000 of Perkin-Elmer from 25 ºC to 200 ºC at 20 ºC/min under flowing nitrogen (N_2) atmosphere. The mass of the PVDF/IL samples was between 5 and 10 mg. For isothermal crystallization experiments, samples were heated to 200 ºC for 5 min and cooled down to the different crystallization temperatures (120 ºC, 140 ºC and 160 ºC) at 90 ºC/min which was the highest cooling rate at which the DSC is kept under control during the whole cooling scan.

Fourier transformed infrared spectroscopy in the attenuated reflection mode was performed using a Nicolet 6700 spectrometer equipped with deuterated triglycine sulfate (DTGS) detector, KBr beam splitter, and horizontal micro-ATR Golden Gate unit (SPECAC) with a diamond crystal enabling isothermal ATR- FTIR measurements at determined temperatures. Small amount of sample was spread on the diamond crystal at room temperature using a spatula, heated to 200 ºC and kept in molten state at 200 ºC for 5 min. Then it was cooled down at 15 ºC/min to selected crystallization temperature. After achieving the required crystallization temperature ATR-FTIR spectra collection was

started. Sixty-four scans with spectral resolution 4 cm^{-1} were coadded to achieve a good signal-to-noise ratio at each isothermal crystallization time.

Optical microscopy (OM) was performed with a Nikon Eclipse E600 microscope, with polarized light, between crossed polarizers, and equipped with a Linkam THMS600 thermostatic plate refrigerated with a flow of cooling air.

3. RESULTS AND DISCUSSION

3.1. Morphological features

Figure 1 shows the FESEM images showing the morphology of the PVDF/[Emim][PF_6] blends with different IL contents. It is worth noting that pristine [Emim][PF_6] crystallizes at temperatures close to room temperature, as it will be shown latter with the DSC thermograms. The typical spherulitic structure of neat PVDF is observed (Figure 1a). This structure is the same as the one observed in the blend with 5 wt% of IL (Figure 1b). Nevertheless, for higher IL contents (25 wt% and 40 wt%), the [Emim][PF_6] crystals clearly appear at the surface of the film.

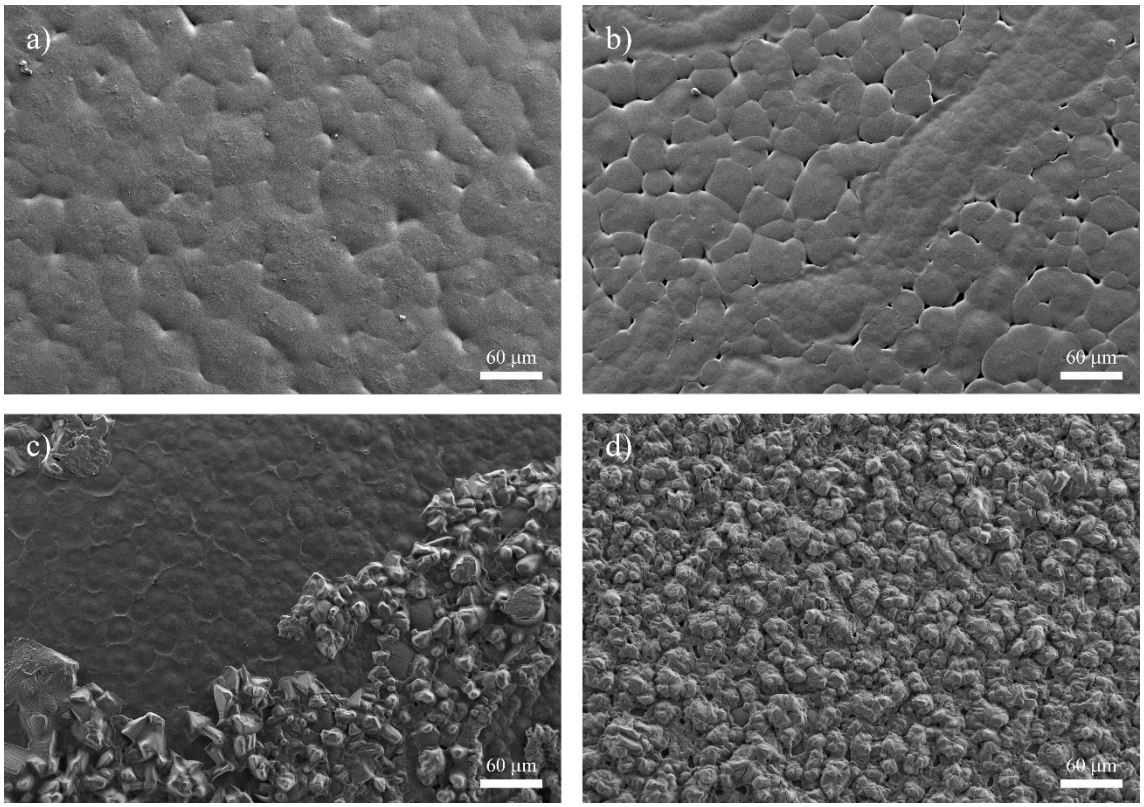

Figure 1. FESEM images at 200x of the surface of the PVDF/IL films. (a) Neat PVDF, (b) 10 wt %, (c) 25 wt%, and (d) 40 wt% IL content.

In the 25wt% blend, regions rich in IL crystals and others with the appearance of the PVDF surface are shown, where the size of the spherulites is smaller than in pure PVDF (Figure 1c). The sample containing 40wt% shows a surface completely covered by [Emim][PF_6].

In order to observe in detail the phase separation, EDS mapping images of the fluoride element and the phosphorus element were observed, as the fluoride and phosphorus elements are present only in the polymer and in the IL, respectively.

Figure 2 shows the EDS mapping images of the fluoride element as a function of the IL content. For higher IL contents (25 wt% and 40 wt%), black areas are observed, demonstrating the presence of IL aggregates. Moreover, these images show that the IL is distributed throughout the sample, proving the phase separation observed in the FESEM images in Figure 1.

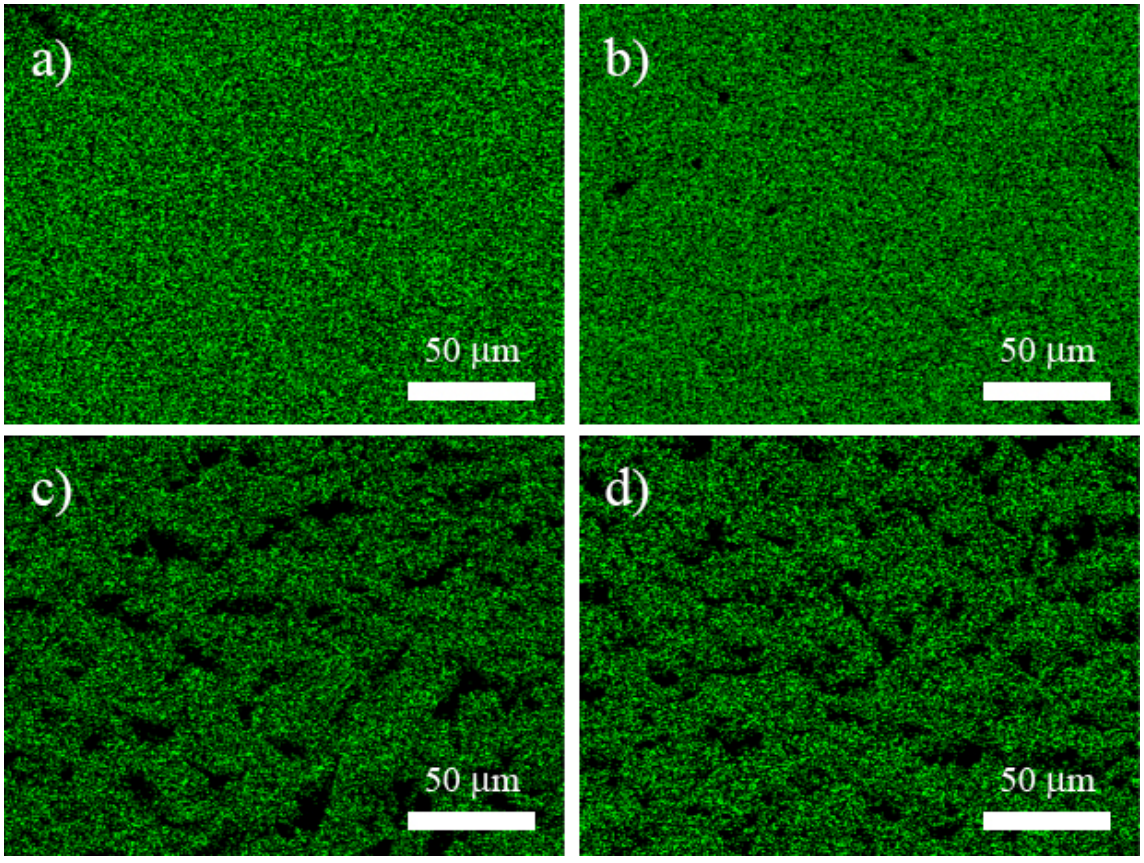

Figure 2. EDS mapping image of the fluoride element of the PVDF/IL films. (a) 5 wt%, (b) 10 wt %, (c) 25 wt%, and (d) 40 wt% IL content.

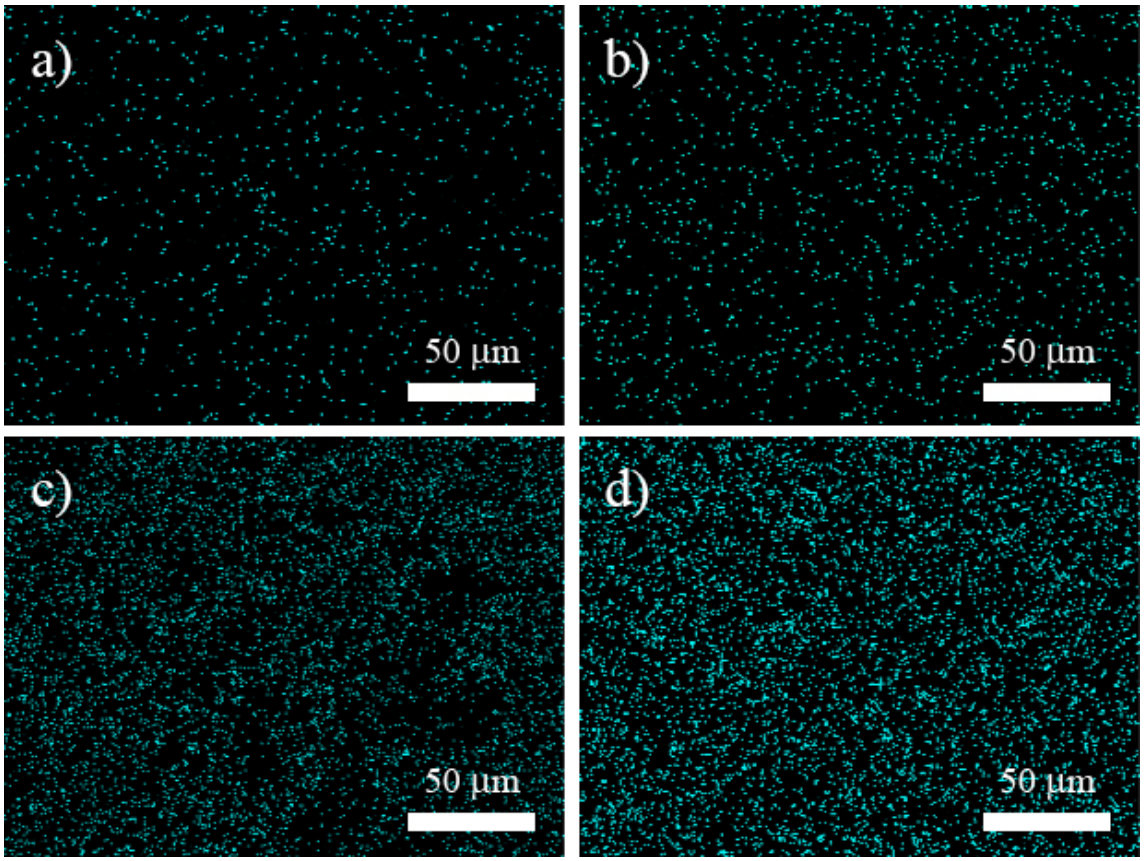

Figure 3. EDS mapping image of the phosphorus element of the PVDF/IL films. (a) 5wt%, (b) 10wt %, (c) 25 wt%, and (d) 40 wt% IL content.

Figure 3 shows the EDS mapping images of the phosphorus element as a function of the IL content, where the intensity of this element increases with increasing IL content. In addition, IL is shown to be distributed throughout the sample.

3.2. Crystallization of [Emim][PF_6] in the blend with PVDF

The DSC thermograms for all samples including pure [Emim][PF_6] for two consecutive heating scans are shown in Figure 4. The second scan was performed after cooling the

sample in the calorimeter at 20 ºC/min. In pure [Emim][PF_6] cooling at 20 ºC/min allows only partial crystallization of the IL. As a consequence, in the heating scan that follows this treatment, a peak of cold crystallization still appears. Then, the melting peak is wider in the second scan, suggesting a crystal size distribution.

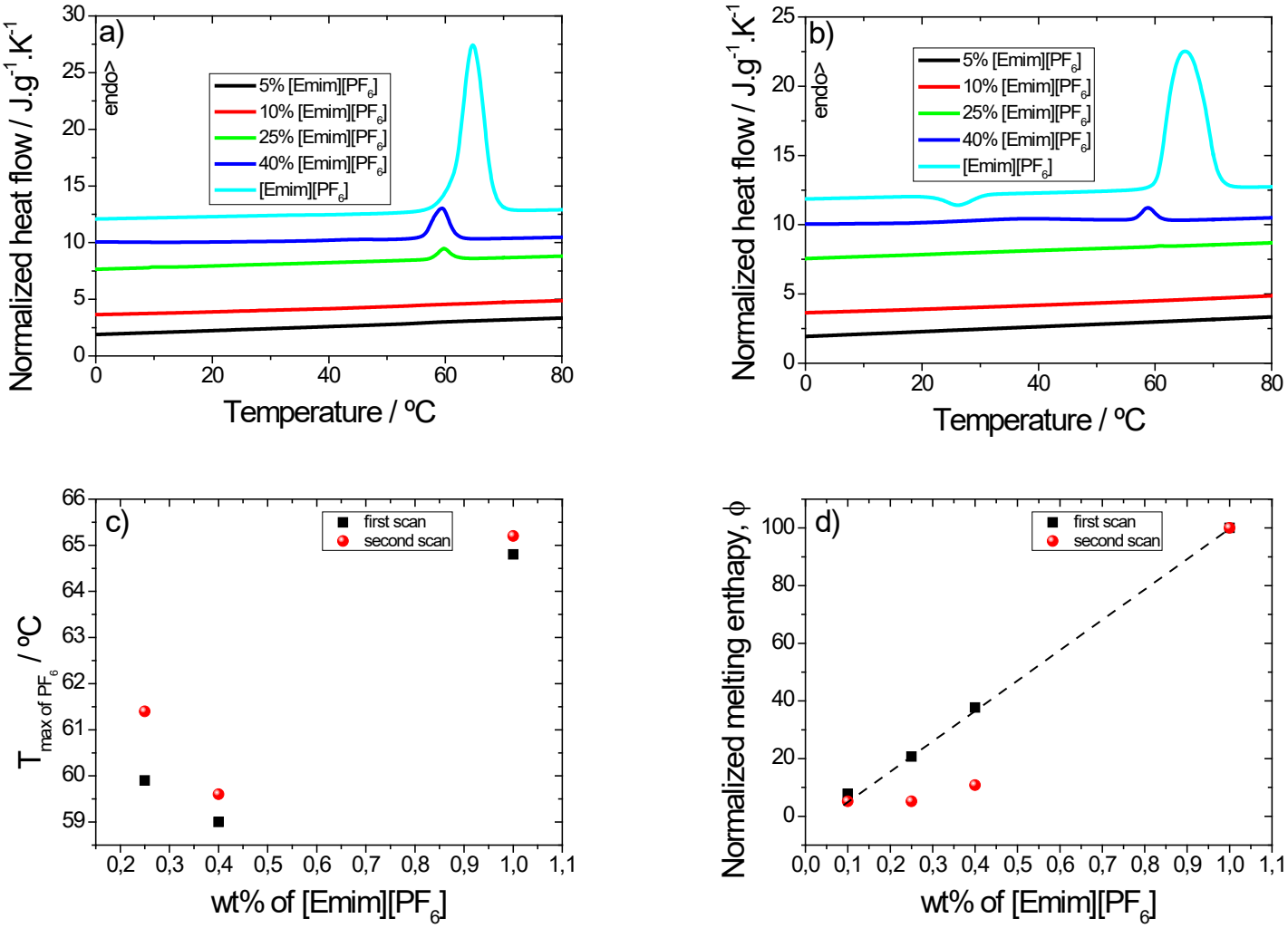

Figure 4. DSC thermogram in the region of the melting behavior of [Emim][PF_6] recorded in the first heating scan (a) and second scan (b). Melting temperature of the IL is shown in (c) and the plot (d) shows the value of φ in equation (1): melting enthalpy expressed as the percentage of the value corresponding to pure [Emim][PF_6].

No significant crystallization or melting processes are observed in the blends with 5wt% and 10wt% of IL. The area of the melting peak in the 25wt% and 40wt% blends, allows to calculate the fraction of IL with the ability to crystallize, that, according to expression (1), is 40± 4%, in the first heating scan (Figure 4d)

$$\varphi = \frac{\Delta H_M}{\Delta H_{[Emim][PF6]}\phi} \text{ x } 100 \quad (1)$$

where ΔH_M is the heat of fusion measured in the scan of the blend, $\Delta H_{[Emim][PF6]}$ is the heat of fusion measured in the pure IL and ϕ is the weight fraction of IL in the blend.

Figure 4 shows the melting temperature and the value of the normalized heat of fusion of the IL as a function of IL content. The melting temperature of the IL in the blend is about 4 ºC below that of pure [Emim][PF_6]. It is worth noting that during melting and crystallization of [Emim][PF_6] in the blend, between 0 and 80 ºC, PVDF crystallites remain unchanged. The IL molecules can distribute either in the space between the lamellae or between the spherulites, homogeneously mixed with the amorphous PVDF chains, or as a separated phase consisting in pure [Emim][PF_6] occupying the inter-spherulitic regions. The decrease in the melting temperature of [Emim][PF_6] over pure [Emim][PF_6] supports the homogeneous mixing of the two components between the PVDF crystals, the amorphous PVDF chains acting as a solute producing the cryoscopic descent. If melting of the IL would take place in a pure IL domain, the melting temperature would be stay as the one of the pure component.

Only a part of the IL molecules has the ability to crystallize from their mixture with the PVDF chains, as seen in Figure 4d. The explanation of this fact also comes from the phase diagram that is deduced from the thermodynamic equilibrium criteria. When a mixture of PVDF and IL with a low IL content is cooled, the equilibrium occurs between the liquid mixture (amorphous phase) and the PVDF crystals. As the amount of crystallized PVDF

increases, the liquid mixture becomes enriched in IL, but IL crystals would not begin to form until an eventual eutectic point was reached. However, before this occurs, the increasing viscosity of the PVDF-IL mixture decreases the ability of the IL molecules to diffuse to form crystals, and finally the vitrification of the amorphous phase totally prevents crystallization. This phenomenon, which means that in mixtures of polymer and a low molecular weight substance only a part of the latter has the ability to crystallize, has been demonstrated in other systems [21].

3.3. PVDF crystallization in the blend with [Emim][PF_6].

Figure 5 shows the melting behavior of PVDF in PVDF/IL blends, where a very different behavior is observed in PVDF/IL blends with 5wt% and 10wt% compared to PVDF/IL blends with 25wt% and 40wt%.

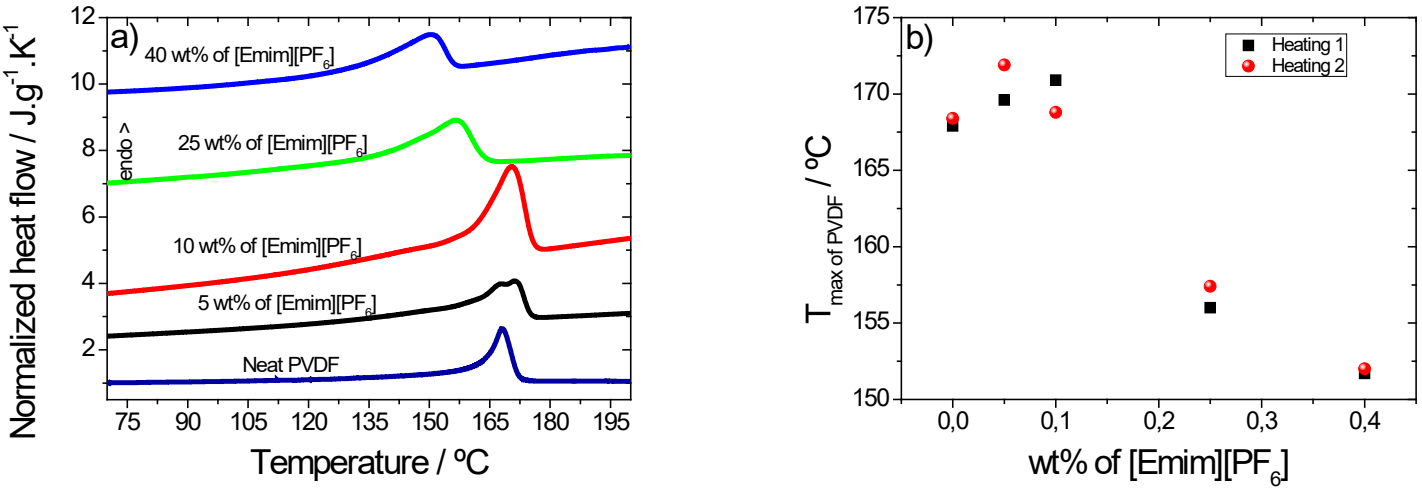

Figure 5. (a) DSC thermogram of the melting region of PVDF measured in the second heating scan and (b) melting temperature as a function [Emim][PF_6] content.

The behavior of the PVDF/IL blends with 5wt% and 10wt% seems to reflect the formation of a crystalline phase with a higher melting temperature than that of the predominant α-phase in PVDF crystallized from the melt. It has been observed in pure

PVDF that the melting temperature of the β-phase is not significantly different from that of the α-phase [5], while that of the γ-phase is of the order of 8 ºC higher when the γ-phase is formed from the melt by isothermal crystallization at high temperature [5, 22]. The effect is clearer in PVDF/IL blends with 5wt%, in which a double melting peak is observed, while PVDF/IL blends with 10wt% shows a single peak but at higher temperatures than in neat PVDF. In an homogeneous blend in which PVDF acts as a solvent while the IL acts as the solute (note that this temperature interval is above the melting temperature of [Emim][PF_6]), the thermodynamic equilibrium predicts a lower melting temperature compared to the pure component. In this temperature range, the observed crystallization and melting processes are related to the process in which PVDF crystals grow from the liquid mixture (Figure 5(b)). The expected behavior is the one observed in PVDF/IL blends with 25wt% and 40wt%. It appears that in PVDF/IL blends with 5wt% or 10wt% the effect of the change in the crystalline phase is above that of the cryoscopic descent. In any case, the effect described in the samples that are crystallized by cooling at constant rate from the melt is difficult to analyze, therefore, in the following, the effect of the IL on isothermal crystallization in a wide range of temperatures will be studied.

PVDF can crystallize from the melt in different crystalline phases depending on the crystallization temperature. It has been reported that the γ phase forms at temperatures above 155 ºC and that its melting temperature is around 7 ºC higher than that of the α and β phases [23]. This phenomenon can be observed when PVDF is crystallized at different crystallization temperatures (T_c), and a heating DSC scan is performed after isothermal crystallization between T_c and 200 ºC, without ever lowering the temperature below T_c. Figure 6a shows such experiments. At temperatures T_c below 150 ºC the heating scan shows a single melting peak (Figure 6a) at a temperature, T_m, that increases gradually with T_c. For higher values of T_c, up to 162 ºC, the melting process breaks down into up

to three endothermic peaks whose temperatures rise with T_c as shown in Figure 6b. They can be associated with the formation of different crystalline phases. While below 150 ºC only the α-phase is formed, at higher temperatures simultaneous formation of α and γ-phases can take place, and even the overlapping of an exothermal taking place during the scan itself cannot be discarded. This phenomenon is similar in the blends of PVDF and the IL, although the number of melting processes and their temperatures depends on the IL content of the blend. Figure 6b shows that in the blend containing 10wt% only two peaks appear, whereas in that containing 40wt% IL only one melting peak is shown (data corresponding to samples containing 5wt% and 25wt% IL are shown as Supplementary material Figure S1). We will come back to these thermograms later.

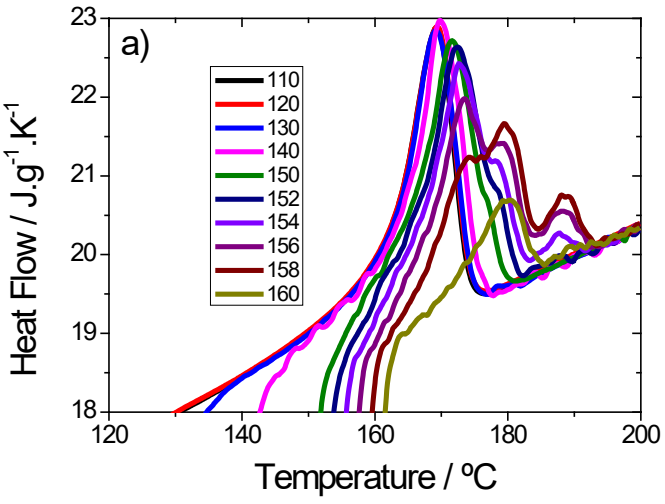

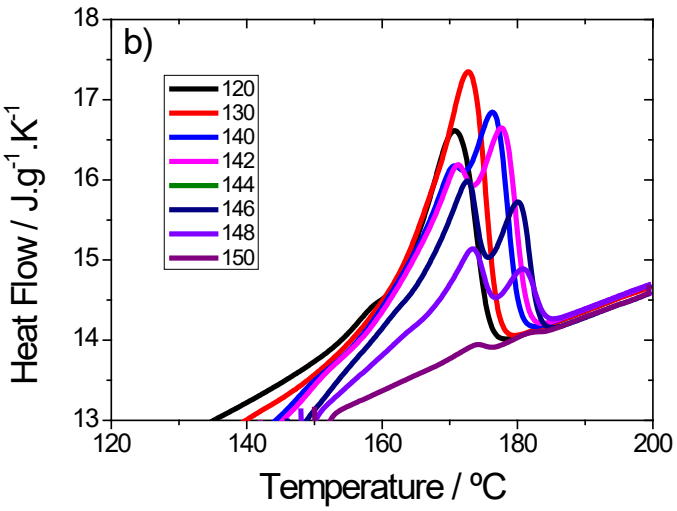

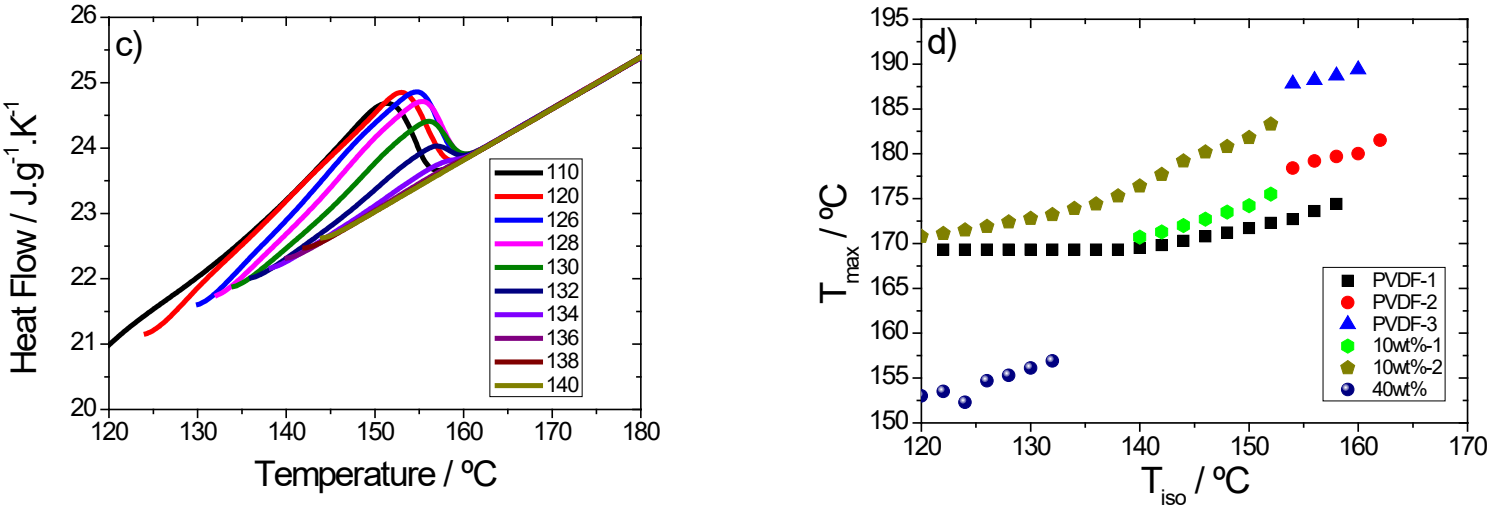

Figure 6. (a) Heating DSC thermograms measured after isothermal crystallization at different crystallization temperatures (indicated in the figure, temperatures in ºC) in neat PVDF, and samples containing 10wt% (b) and 40wt% (c). (d) Maximum melting temperature as a function of isothermal temperature.

To study the formation of the different crystalline phases in the blends, the FTIR spectra measured during the isothermal crystallization process at different temperatures is analyzed. The spectrum measured at 200 ºC is also shown as representative of the PVDF liquid state. Figure 7a shows the FTIR spectra as a function of time at a crystallization temperature of 160 ºC where the evolution of the characteristic peaks of the α-phase at 615, 763, 796 and 976 cm^{-1} can be observed. A peak also appears at 840 cm^{-1} with a small intensity that has been assigned to the β-phase but with the possible contribution of the γ-phase [24].

On the other hand, the peaks at 872, 978, 1067 and 1398 cm^{-1} are associated with vibrations common to the different crystalline phases [24]. All of them, except for the band at 1067 cm^{-1}, also appear in the molten polymer. The peak at 1067 cm^{-1} is characteristic of the crystalline order and it can be seen how the peak grows with crystallization time at 160ºC (Figure 7a), and that it does not seem to present any peculiarities in the different

samples, as it also appears in the samples in which the α-phase practically does not appear. The β-phase content of neat PVDF is 33% [17].

At 140 ºC, the FTIR spectrum does not depend on the crystallization time because most of the crystalline fraction develops in a very short time. (Supplementary material Figure S2).

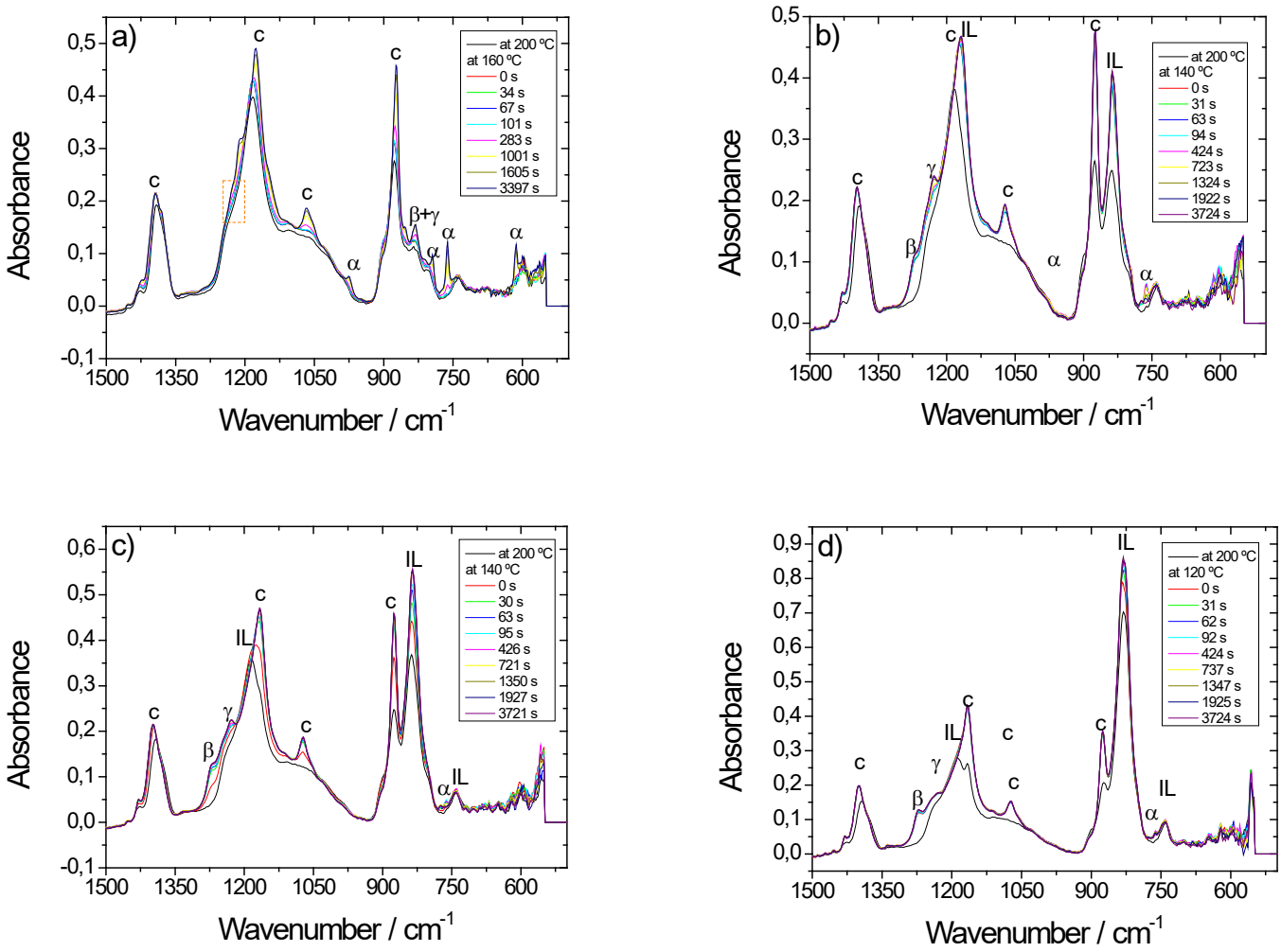

Figure 7. FTIR spectra of PVDF/IL films measured as a function of time. a) Neat PVDF during isothermal crystallization at 160 ºC. b) 5wt% and c) 10wt% IL during isothermal crystallization at 140 ºC. d) 40wt% IL during isothermal crystallization at 120 ºC.

It is interesting to note that in addition to the characteristic peaks of the α and β-phases mentioned above, there are also small signs at 811 cm^{-1} and a shoulder in the region around 1234 cm^{-1} that reveal the presence of the crystalline γ-phase differentiating it from the β-phase. In all of this, our results agree with what could be expected from the literature [17].

FTIR spectra of all PVDF/[Emim][PF_6] blends as a function of time for the crystallization temperature at 120 or 140 ºC are shown in Figure 7b to 7d. It can be observed that the

addition of 5wt% of IL to the polymer matrix completely changes the crystallization behavior (Figure 8a) when compared to neat PVDF (Figure 7a). All the α-phase characteristic bands disappear with the only exception of a small peak at 763 cm^{-1}.

The crystallization temperature of 140 ºC has been selected in Figure 8 in the case of PVDF/[Emim][PF_6] with 5 wt% and 10 wt% that showed melting peaks in the heating thermograms at temperatures very close to pure PVDF. Nevertheless, at that temperature nearly no crystallization takes place in the case of PVDF/[Emim][PF_6] with 25 wt% and 40 wt%, thus the spectra at 120 ºC are shown in these samples.

Regardless to IL content, all PVDF/[Emim][PF_6] blends show the characteristic peaks at 740, 816 and 1164 cm^{-1} that correspond to ring HCCH sym bend, CCH bend and CH_3(N) HCH bend, respectively [25].

Also, it is observed a clear shift of the vibration peaks of the IL in the PVDF/[Emim][PF_6] blends that can demonstrate the interaction between [Emim][PF_6] anion or cation with the PVDF chain segments. Thus, in Table 1 the wave numbers of the three most intense peaks of [Emim][PF_6] are listed, which are the ones that later in the blends are also appreciable.

Table 1. Wavenumbers (cm^{-1}) of the characteristic peaks of [Emim][PF_6] in all PVDF/[Emim][PF_6] blends

[Emim][PF_6]	5wt%	10wt%	25wt%	40wt%
1164	1168	1164	1164	1164
816	840	838	832	822
740/750	740	740	740	740

The most significant difference is the shift of the 816 cm^{-1} peak, which in PVDF/[Emim][PF_6] with 5wt% shifts to 840 cm^{-1} and approaches that of pure [Emim][PF_6] as the IL content in the blends increases.

The peaks of the IL hide the most significant region of the spectrum associated with the polar β-phase, but in the region between 1200 and 1300 cm^{-1}, where it is very significant

to differentiate β-phase and γ-phase, it is possible to see the appearance of the peaks at about 1230 cm^{-1} corresponding to the γ-phase, and about 1270 cm^{-1} of the β-phase [24]. It seems that the isothermal crystallization of the PVDF/[Emim][PF_6] blends clearly forms a mixture of these two phases. As the IL content increases, these peaks clearly increase in intensity and the small signs of α-phase disappear almost completely (Figure 7). The scheme 1 shows the electrostatic interaction between the IL and the PVDF polymer chains responsible for the nucleation of the β- and γ-phases.

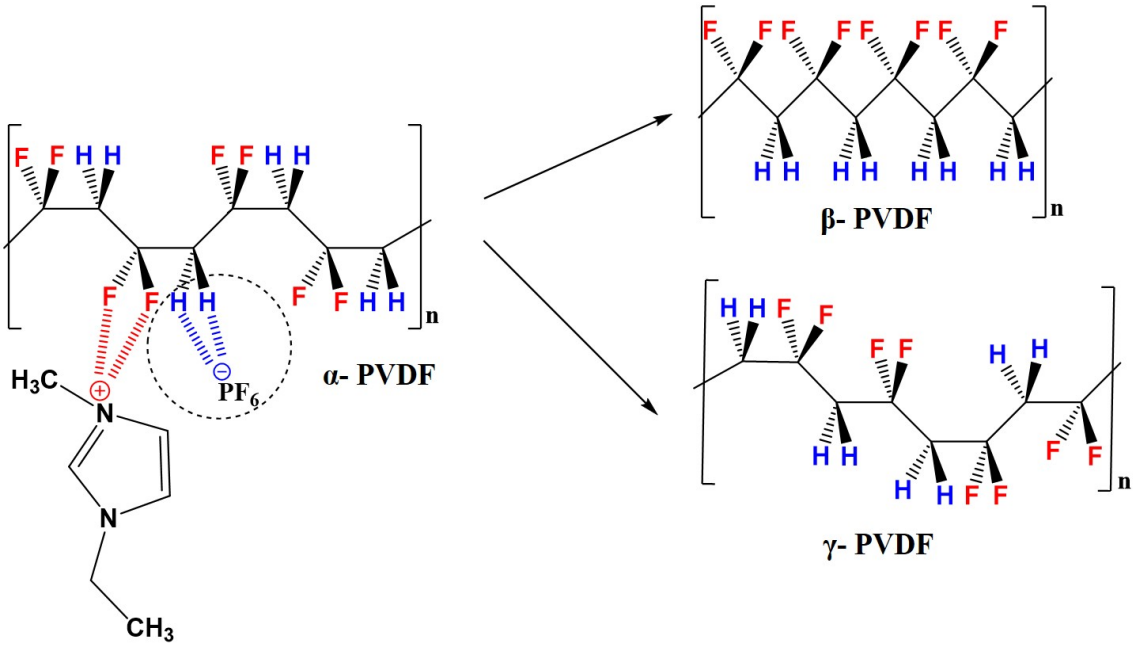

Scheme 1. Schematic representation of the electrostatic interaction between the IL and the PVDF polymer chains.

The reason for the nucleation of the polar phases is due to the electrostatic interactions between protons in the CH_2 groups and anions in the ionic liquid, which are stronger due to the less stereochemical impediment compared to the CF_2 groups and the cations [26].

It is interesting to see that although in PVDF/[Emim][PF_6] with 5wt% or 10wt% the melting temperature of PVDF does not decrease with respect to that of neat PVDF as would be expected when IL is added as a solute in the liquid mixture, in isothermal crystallization there is a clear effect of cryoscopic descent. In fact, while for neat PVDF

the sample has crystallization up to 162ºC, in PVDF/[Emim][PF_6] with 5 wt% there are no traces of exothermic process in the isotherms above 158 ºC or in PVDF/[Emim][PF_6] with 10 wt% above 154 ºC (results not shown).

In order to demonstrate this effect, Figure 8a shows the crystallization isotherms in all PVDF/[Emim][PF_6] blends, selecting for each sample the crystallization temperature for which the maximum of the exotherm occurs at the crystallization time of 30 s (Figure S3 in supplementary material shows the set of isotherms recorded in the sample containing 10wt% IL as a representative example of the results obtained for the rest of the blends). In this way, we compare the process at temperatures at which the crystallization rate is the same in the different PVDF/[Emim][PF_6] blends. The broadening of the peak is clearly observed in the PVDF/[Emim][PF_6] blends with 25 wt% and 40 wt% content that has to do with the equilibrium process between the solid phase consisting of the pure PVDF crystal and the liquid phase consisting of a mixture of amorphous PVDF chains and the ionic liquid.

When the heating scan is carried out immediately after the crystallization has finished and without lowering the temperature, the evolution with the [Emim][PF_6] content is clearly observed (Figure 8b).

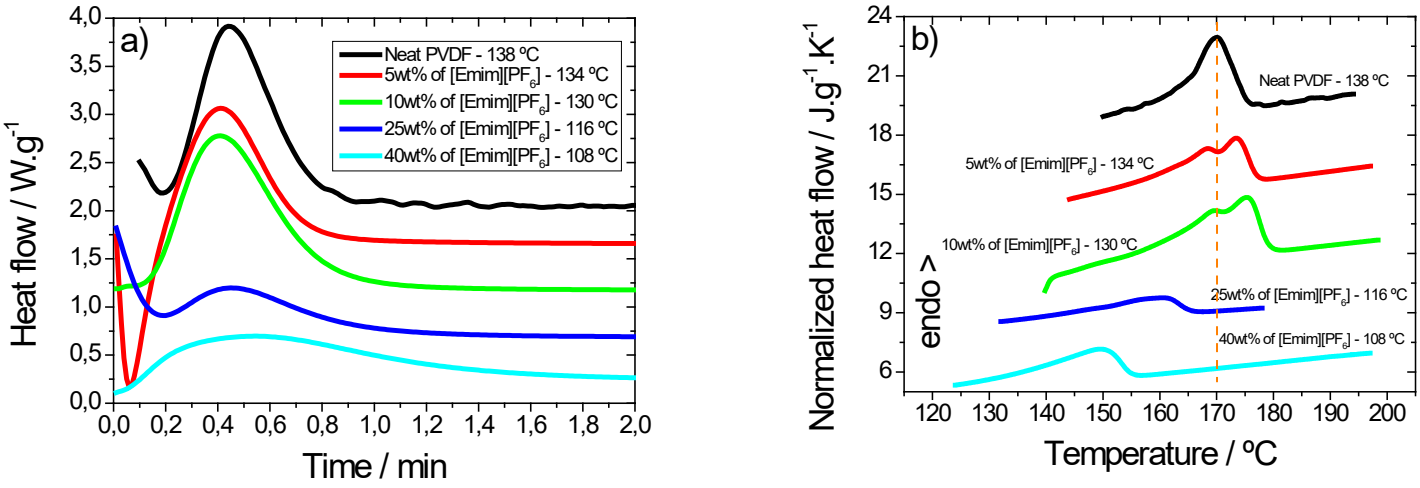

Figure 8. (a) Isothermal crystallization peaks where the maximum exothermic peak is 30 seconds and (b) melting peaks behavior for all PVDF/[Emim][PF_6] blends.

At that temperature, in pure PVDF only one melting peak appears, which would be the one corresponding to the α-phase, which has already been seen to be the one that is formed in the greatest proportion at those temperatures that are too low for it to form γ-phase. However, in the PVDF/[Emim][PF_6] blends with 5 wt% and 10 wt%, a double peak is observed that can be associated with the melting of the two phases, β and γ, present in the material that have temperatures separated by five or six degrees.

Considering this effect, optical microscopy with crossed polarizers was used to follow isothermal crystallization. Figure 9 a-c shows that the spherulite structure observed in neat PVDF is maintained in the PVDF/[Emim][PF_6] blends with 10wt% and 25wt% IL content, although birefringence is less intense what can be due to the presence of the liquid [Emim][PF_6] mixed with the PVDF amorphous chains.

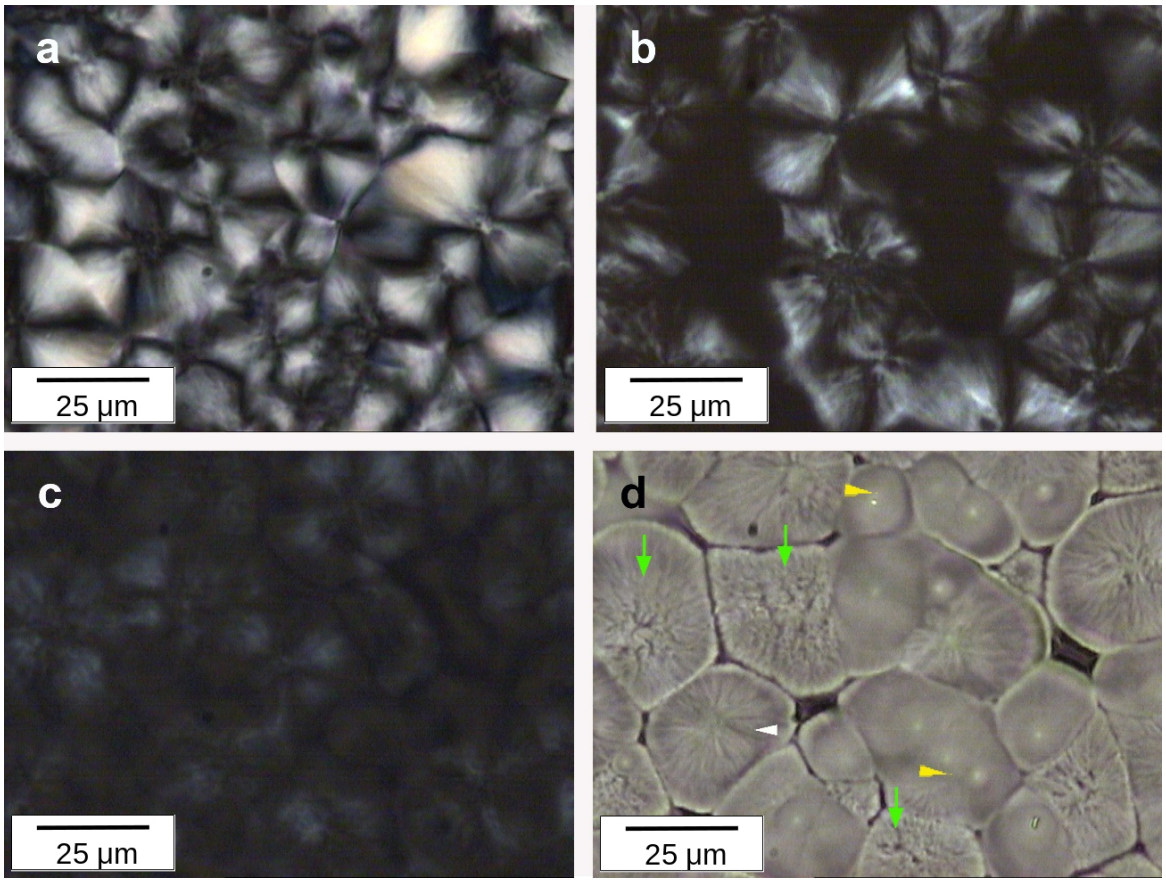

Figure 9. Image captured with the polarized light optical microscope with crossed polarizers in neat PVDF (a) and PVDF/[Emim][PF_6] blends containing 10 wt% IL (b) and 25 wt% IL (c) after isothermal crystallization at the same temperatures than in Figure 9. The image recorded with non-crossed polarizers in the sample containing 25% IL is shown in figure 10-d.

Figure 9d shows the picture recorded with aligned polarizers in the sample containing 25% IL. There appear different spherulite structures like those shown by the white and green arrows and the drops of liquid [Emim][PF_6] marked by the yellow arrows (note that the crystallization temperature is above the melting point of the IL).

4. CONCLUSIONS

Blends of PVDF with the ionic liquid [Emim][PF_6] were produced in order to study their crystallization kinetics as a function of temperature when crystallized from the melt. Crystallization kinetics has been monitored using FTIR spectroscopy and were characterized by differential scanning calorimetry. Also, the microstructure of the blends has been analyzed by scanning electron and optical microscopies.

In mixtures of PVDF and the IL [Emim][PF_6], isothermal crystallization from the melt in the crystallization temperature interval between 120 and 162 ºC yields PVDF crystallites in the β and γ electroactive phases, while the formation of α–phase crystals is nearly suppressed. The [Emim][PF_6] remains liquid when mixed with the amorphous PVDF chains and crystallizes on cooling from this mixture in a range of temperatures that depend on the blend composition and the cooling rate. During heating, melting temperature is lower in the blends than in the pure [Emim][PF_6] due to the cryoscopic descent supporting the homogeneous mixing in the amorphous phase. The [Emim][PF_6] crystals can be observed at the surface of the blend films together with the PVDF spherulites, confirming solid phases separation at room temperature.

ASSOCIATED CONTENT

Supporting Information

PVDF crystallization in the blend with [Emim][PF_6], FTIR spectrum at 140 ºC for neat PVDF and crystallization isotherms for PVDF/[Emim][PF_6] blend with 10 wt% IL content

AUTHOR INFORMATION

Corresponding Author

cmscosta@fisica.uminho.pt (C. M. Costa),

Author Contributions

The manuscript was written through contributions of all authors. All authors have given approval to the final version of the manuscript

Notes

The authors declare no competing financial interest.

ACKNOWLEDGEMENTS

This work was supported by the Portuguese Foundation for Science and Technology (FCT) in the framework of the Strategic Funding UID/FIS/04650/2019. The authors thank FEDER funds through the COMPETE 2020 Programme and National Funds through FCT under the projects PTDC/BTM-MAT/28237/2017, PTDC/EEI-SII/5582/2014 and PTDC/FIS-MAC/28157/2017. D.M.C. thank the FCT for grant SFRH/BPD/121526/2016 and C.M.C for the Investigator FCT Contract 2020.04028.CEECIND. The work of the Spanish groups has been funded by the Spanish State Research Agency (AEI) through the PID2019-106099RB-C41 / AEI / 10.13039/501100011033 project and from the Basque Government Industry and Education Departments under the ELKARTEK and PIBA (PIBA-2018-06) programs, respectively. CIBER-BBN is an initiative funded by the VI National R&D&I Plan 2008–2011, Iniciativa Ingenio 2010, Consolider Program. CIBER Actions are financed by the Instituto de Salud Carlos III with assistance from the European Regional Development Fund.

REFERENCES

1. Dilberoglu, U. M.; Gharehpapagh, B.; Yaman, U.; Dolen, M. The Role of Additive Manufacturing in the Era of Industry 4.0. *Procedia Manufacturing* **2017,** *11*, 545-554.

2. Oliveira, J.; Correia, V.; Castro, H.; Martins, P.; Lanceros-Mendez, S. Polymer-based smart materials by printing technologies: Improving application and integration. *Additive Manufacturing* **2018,** *21*, 269-283.

3. Tressler, J. F.; Alkoy, S.; Dogan, A.; Newnham, R. E. Functional composites for sensors, actuators and transducers. *Composites Part A: Applied Science and Manufacturing* **1999,** *30*, 477-482.

4. Carvalho, E.; Fernandes, L.; Costa, C. M.; Lanceros-Méndez, S. Piezoelectric Polymer Composites for Sensors and Actuators. In *Reference Module in Materials Science and Materials Engineering*, Elsevier: **2020**.

5. Martins, P.; Lopes, A. C.; Lanceros-Mendez, S. Electroactive phases of poly(vinylidene fluoride): Determination, processing and applications. *Progress in Polymer Science* **2014,** *39*, 683-706.

6. Xin, Y.; Sun, H.; Tian, H.; Guo, C.; Li, X.; Wang, S.; Wang, C. The use of polyvinylidene fluoride (PVDF) films as sensors for vibration measurement: A brief review. *Ferroelectrics* **2016,** *502*, 28-42.

7. Nalwa, H. S. RECENT DEVELOPMENTS IN FERROELECTRIC POLYMERS. *Journal of Macromolecular Science, Part C* **1991,** *31*, 341-432.

8. Nalwa, H. S. *Ferroelectric Polymers: Chemistry: Physics, and Applications*. Taylor & Francis: **1995**.

9. Ribeiro, C.; Costa, C. M.; Correia, D. M.; Nunes-Pereira, J.; Oliveira, J.; Martins, P.; Gonçalves, R.; Cardoso, V. F.; Lanceros-Méndez, S. Electroactive poly(vinylidene

fluoride)-based structures for advanced applications. *Nature Protocols* **2018,** *13*, 681-704.

10. Lovinger, A. J. Crystalline transformations in spherulites of poly(vinylidene fluoride). *Polymer* **1980,** *21*, 1317-1322.

11. Matsushige, K.; Nagata, K.; Imada, S.; Takemura, T. The II-I crystal transformation of poly(vinylidene fluoride) under tensile and compressional stresses. *Polymer* **1980,** *21*, 1391-1397.

12. Sencadas, V.; Lanceros-Mendez, S.; Filho, R. G.; Chinaglia, D. L.; Pouzada, A. S. In *Influence of the processing conditions and corona poling on the morphology of /spl beta/-PVDF*, 2005 12th International Symposium on Electrets, 11-14 Sept. 2005; **2005**; pp 161-164.

13. Correia, D. M.; Fernandes, L. C.; Martins, P. M.; García-Astrain, C.; Costa, C. M.; Reguera, J.; Lanceros-Méndez, S. Ionic Liquid–Polymer Composites: A New Platform for Multifunctional Applications. *Advanced Functional Materials* **2020,** *30*, 1909736.

14. Introduction: Ionic Liquids. *Chemical Reviews* **2017,** *117*, 6633-6635.

15. Dong, K.; Liu, X.; Dong, H.; Zhang, X.; Zhang, S. Multiscale Studies on Ionic Liquids. *Chemical Reviews* **2017,** *117*, 6636-6695.

16. Correia, D. M.; Sabater i Serra, R.; Gómez Tejedor, J. A.; de Zea Bermudez, V.; Andrio Balado, A.; Meseguer-Dueñas, J. M.; Gomez Ribelles, J. L.; Lanceros-Méndez, S.; Costa, C. M. Ionic and conformational mobility in poly(vinylidene fluoride)/ionic liquid blends: Dielectric and electrical conductivity behavior. *Polymer* **2018,** *143*, 164-172.

17. Correia, D. M.; Costa, C. M.; Lizundia, E.; Sabater i Serra, R.; Gómez-Tejedor, J. A.; Biosca, L. T.; Meseguer-Dueñas, J. M.; Gomez Ribelles, J. L.; Lanceros-Méndez, S.

Influence of Cation and Anion Type on the Formation of the Electroactive β-Phase and Thermal and Dynamic Mechanical Properties of Poly(vinylidene fluoride)/Ionic Liquids Blends. *The Journal of Physical Chemistry C* **2019,** *123*, 27917-27926.

18. Correia, D. M.; Costa, C. M.; Rodríguez-Hernández, J. C.; Tort Ausina, I.; Biosca, L. T.; Torregrosa Cabanilles, C.; Meseguer-Dueñas, J. M.; Lanceros-Méndez, S.; Gomez Ribelles, J. L. Effect of Ionic Liquid Content on the Crystallization Kinetics and Morphology of Semicrystalline Poly(vinylidene Fluoride)/Ionic Liquid Blends. *Crystal Growth & Design* **2020,** *20*, 4967-4979.

19. Zhang, H.; Shi, W.; Cheng, H.; Chen, S.; Wang, L. Effect of ionic liquid on crystallization kinetics and crystal form transition of poly(vinylidene fluoride) blends. *Journal of Thermal Analysis and Calorimetry* **2018,** *132*, 1153-1165.

20. Roy, A.; Dutta, B.; Bhattacharya, S. Electroactive phase nucleation and non-isothermal crystallization kinetics study in [DEMM][TFSI] ionic liquid incorporated P(VDF-HFP) co-polymer membranes. *Journal of Materials Science* **2016,** *51*, 7814-7830.

21. Salmerón Sánchez, M.; Monleón Pradas, M.; Gómez Ribelles, J. L. Thermal transitions of benzene in a poly(ethyl acrylate) network. *Journal of Non-Crystalline Solids* **2002,** *307-310*, 750-757.

22. Gregorio Jr., R. Determination of the α, β, and γ crystalline phases of poly(vinylidene fluoride) films prepared at different conditions. *Journal of Applied Polymer Science* **2006,** *100*, 3272-3279.

23. Gregorio, R.; CapitãO, R. C. Morphology and phase transition of high melt temperature crystallized poly(vinylidene fluoride). *Journal of Materials Science* **2000,** *35*, 299-306.

24. Cai, X.; Lei, T.; Sun, D.; Lin, L. A critical analysis of the α, β and γ phases in poly(vinylidene fluoride) using FTIR. *RSC Advances* **2017,** *7*, 15382-15389.

25. Talaty, E. R.; Raja, S.; Storhaug, V. J.; Dölle, A.; Carper, W. R. Raman and Infrared Spectra and ab Initio Calculations of C2-4MIM Imidazolium Hexafluorophosphate Ionic Liquids. *The Journal of Physical Chemistry B* **2004,** *108*, 13177-13184.

26. Wang, F.; Lack, A.; Xie, Z.; Frübing, P.; Taubert, A.; Gerhard, R. Ionic-liquid-induced ferroelectric polarization in poly(vinylidene fluoride) thin films. *Applied Physics Letters* **2012,** *100*, 062903.

TOC-Synopsis page

Manuscript title: Crystallization Monitoring of Semicrystalline Poly(vinylidene) Fluoride/ 1-ethyl-3-methylimidazolium Hexafluorophosphate [Emim][PF_6] Ionic Liquid Blends

Author list: Daniela M. Correia, Carlos M. Costa, José C. Rodríguez Hernández, Isabel Tort-Ausina, Laura Teruel Biosca, Constantino Torregrosa Cabanilles, José M. Meseguer-Dueñas, Ivan Krakovsky, Senentxu Lanceros-Méndez, José Luis Gómez Ribelles

TOC graphic

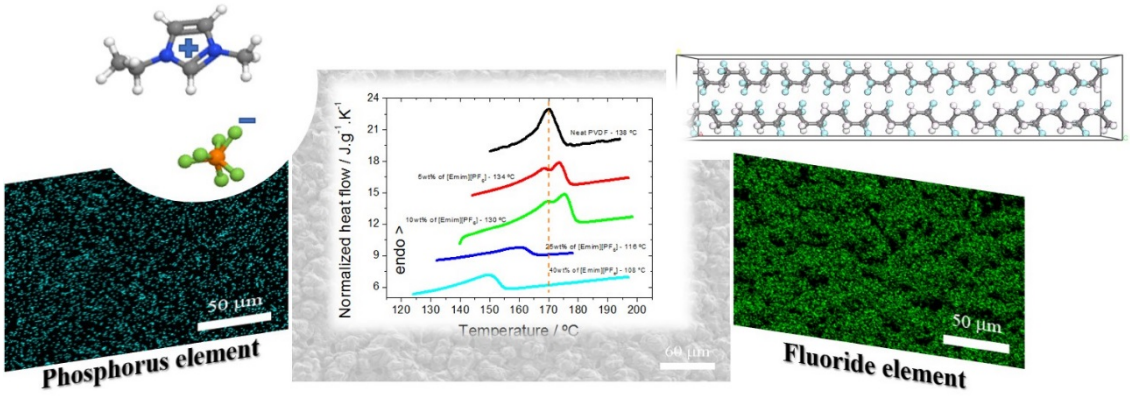

Synopsis:

The crystallization kinetics of PVDF blended with the IL (1-ethyl-3-methylimidazolium hexafluorophosphate [Emim][PF_6]) has been investigated by Fourier transform infrared spectroscopy (FTIR) and Differential Scanning Calorimetry (DSC) at different isothermal crystallization temperatures. PVDF morphology and crystalline phase are affected by the addition of IL, the IL being mixed with the PVDF amorphous chains.